

2014

# High-Resolution Event-Based Data at Diamond Interchanges: Performance Measures and Optimizing Ring Displacement

Alexander M. Hainen

*Purdue University, ahainen@eng.ua.edu*

Amanda L. Stevens

*Indiana Department of Transportation, amilynn1107@yahoo.com*

Richard S. Freije

*Purdue University, rfreije@indot.in.gov*

Christopher M. Day

*Purdue University, cmday@purdue.edu*

James R. Sturdevant

*INDOT, jsturdevant@indot.in.gov*

*See next page for additional authors*

Follow this and additional works at: <http://docs.lib.purdue.edu/civeng>



Part of the [Civil Engineering Commons](#)

Hainen, Alexander M.; Stevens, Amanda L.; Freije, Richard S.; Day, Christopher M.; Sturdevant, James R.; and Bullock, Darcy M., "High-Resolution Event-Based Data at Diamond Interchanges: Performance Measures and Optimizing Ring Displacement" (2014). *Lyles School of Civil Engineering Faculty Publications*. Paper 13. <http://docs.lib.purdue.edu/civeng/13>

This document has been made available through Purdue e-Pubs, a service of the Purdue University Libraries. Please contact [epubs@purdue.edu](mailto:epubs@purdue.edu) for additional information.

---

**Authors**

Alexander M. Hainen, Amanda L. Stevens, Richard S. Freije, Christopher M. Day, James R. Sturdevant, and Darcy M. Bullock

# **High-Resolution Event-Based Data at Diamond Interchanges: Performance Measures and Optimizing Ring Displacement**

Alexander M. Hainen  
Purdue University  
550 Stadium Mall Drive, West Lafayette, IN 47907-2051  
Phone: 765-496-7314 Fax: 765-494-0395  
Email: ahainen@purdue.edu

Amanda L. Stevens  
Indiana Department of Transportation  
8620 East 21st Street, Indianapolis, IN 46219  
Phone: 317-796-2661 Fax: 317-898-0897  
Email: astevens@indot.in.gov

Richard S. Freije  
Purdue University  
550 Stadium Mall Drive, West Lafayette, IN 47907-2051  
Phone: 765-496-7314 Fax: 765-494-0395  
Email: rsfreije@purdue.edu

Christopher M. Day  
400 Centennial Mall Drive, West Lafayette, IN 47907  
West Lafayette, IN 47907-2051  
Phone: 765-494-9601 Fax: 765-494-0395  
Email: cmday@purdue.edu

James R. Sturdevant  
Indiana Department of Transportation  
8620 East 21st Street, Indianapolis, IN 46219  
Phone: 317-796-2661 Fax: 317-898-0897  
Email: jsturdevant@indot.in.gov

## **Corresponding author:**

Darcy M. Bullock  
Purdue University  
400 Centennial Mall Drive, West Lafayette, IN 47907  
Phone: 765-496-2226 Fax: 765-494-0395  
Email: darcy@purdue.edu

November 13, 2013

**TRB Paper 14-0298**

Word Count: 4,310 words + 12 x 250 words/Figure-Table = 4,310 + 3,000 = **7,310**

**ABSTRACT**

Signalized diamond interchanges are unique pairs of intersections characterized by interlocked left turns and relatively close spacing between ramps. A diamond interchange has four external entry points (origins) and four external exit points (destinations). To effectively operate a diamond interchange, it is critical to examine the external origin-destination paths and evaluate their impact on the interior storage and progression. This paper describes a series of performance measures derived from high-resolution signal controller data that can be used to 1) qualitatively and quantitatively assess the quality of progression of the interior movements; and 2) optimize the internal offset to improve traffic flows within the interchange. Additional performance measures for identifying internal and ramp queuing are also discussed. The paper concludes by recommending that the graphical performance measures be integrated into controller front panel displays and central systems to assist engineers in tuning and maintaining efficient operation of diamond interchanges.

## INTRODUCTION

Signalized diamond interchanges are unique pairs of intersections characterized by interlocked left turns and relatively close spacing between ramps. There are over 5 decades of literature on signalizing diamond interchanges oriented toward phase sequencing and timing (1). More recently the literature has developed to consider modern dual-ring controllers and discussed strategies for implementing “3 Phase”, “4 Phase” and ring lag (2). Most of the performance measures reported in the literature use delay, based upon mathematical models, simulation, or floating car studies (3). There is general consensus in the literature that empirical performance measures are needed by practitioners to answer the following questions (4):

1. Are the off-ramps queuing to the point that they impede freeway traffic? (5)
2. Are the diamond interior approaches queuing to the point that they spill back and impede the adjacent intersection movements?
3. Is there reasonable progression through both signals of the diamond interchange for the four external movements?

All three items above are affected by split allocation, but items 2 and 3 also rely heavily on the offset between intersections. This paper discusses how high resolution controller event data can be analyzed to provide performance measures regarding items 2 and 3 and use them as an optimization objective function. High-resolution event-based data (6) (7) had been collected continuously at this interchange for over a year as part of an effort to monitor over 125 controllers in Indiana over low bandwidth commercial cellular service. This data includes every phase state change and vehicle detection event (among other controller events) to the nearest tenth of a second using a data logging utility running in the controller firmware.

## DIAMOND PHASING AND OVERLAPS ON A SINGLE CONTROLLER

Early signalized diamond interchange literature focuses on interval-based timings/controllers (8). In the last two decades, there has been an evolving trend towards controlling both intersections with a single controller using dual rings and overlaps (9) (10) (11). Figure 1 shows an example single controller diamond interchange at I-465 and SR-37 on the south side of Indianapolis, Indiana (Figure 1). Each ring in the dual ring structure controls one intersection, and ring displacement (ring lag) allows the coordinated movements in each ring to be offset as if they are independent intersections. Because each intersection is controlled by one ring, all movements in Ring 1 are compatible with Ring 2. Ring 1 is assigned to the south intersection with the following structure (Figure 1b detail):

- **Phase 1:** Southbound Left (from the internal approach to the freeway on-ramp)
- **Phase 2:** Northbound Thru (from the south external approach)
- **Phase 3:** Eastbound Left & Right (from the exit ramp approach)
- **Overlap-D:** Southbound Thru (from the internal approach). When phase 1 or phase 2 is active, overlap-D will also be active.

Similarly, the north intersection is handled by Ring 2 (Figure 1a detail):

- **Phase 5:** Northbound Left (from the internal approach to the freeway on-ramp)
- **Phase 6:** Southbound Thru (from the north external approach)

- **Phase 7:** Westbound Left & Right (from the exit ramp approach)
- **Overlap-H:** Northbound Thru (from the internal approach). When phase 5 or phase 6 is active, overlap-H will also be active.

Figure 2 shows the AM Peak, Off Peak, and PM Peak coordination patterns used at this interchange, and how the ring displacement (RD) concept works. The ring displacement parameter is effectively an offset between the two “T”-intersections; it controls when vehicles leaving one intersection will arrive at the next intersection. The ring displacement is the amount of time from the start of the coordinated phase in ring 1 (the south intersection) to the start of the coordinated phase in ring 2 (north intersection). In Figure 2a, the coordinated movements are phase 2 and phase 6, as indicated by the asterisks. The ring displacement value of 42 seconds indicates that phase 6 will begin 42 seconds after the start of phase 2. Ring displacement can range between 0 and  $(1 - C)$ , where  $C$  is the cycle length (80 seconds for pattern 1 in Figure 2a), similar to an offset between two independent controllers. In pattern 1, there are 6 intervals of operation depicted in the callout pictograms of Figure 2a including:

- EB exit ramp (phase 3) at the south intersection and NBL (phase 5) & NBT (OL-H) at the north intersection.
- EB exit ramp (phase 3) at the south intersection and SBT (phase 6) & NBT (OL-H) at the north intersection.
- SBL (phase 1) & SBT (OL-D) at the south intersection and SBT (phase 6) & NBT (OL-H) at the north intersection.
- SBL (phase 1) & SBT (OL-D) at the south intersection and WB exit-ramp (phase 7) at the north intersection.
- NBT (phase 2) & SBT (OL-D) at the south intersection and WB exit ramp (phase 7) at the north intersection.
- NBT (phase 2) & SBT (OL-D) at the south intersection and NBL (phase 5) & NBT (OL-H) at the north intersection.

A similar breakdown of intervals is shown pictorially for pattern 2 (Figure 2b) and pattern 3 (Figure 2c). It is important to note that for pattern 2 in Figure 2b, phase 5 is the coordinated phase for the north intersection (noted by the asterisk in Ring 2) due to heavy NBL/NB traffic and thus the ring displacement is the amount of time between the start of phase 2 and the start of phase 5. Table 1 summarizes when each pattern is used. This same methodology can be applied to interchanges with two controllers, although the labeling convention of phases or intervals changes slightly.

## DIAMOND INTERCHANGE MOVEMENTS

A diamond interchange has four external entry points (origins) and four external exit points (destinations). To effectively operate a diamond interchange, it is critical to examine the external origin-destination paths and to evaluate their impact on the interior storage and progression. Considering the interior southbound approach of the south intersection (Figure 1), traffic arriving upstream from the north intersection can come from one of two origins:

- **Origin 1:** The southbound thru movement (phase 6) from the external approach (Figure 3a)
- **Origin 2:** The westbound left movement (phase 7) from the exit ramp (Figure 3b)

Furthermore, these vehicles can only leave the south intersection through one of two movements:

- **Destination 1:** The southbound thru movement (overlap-D) from the internal approach
- **Destination 2:** The southbound left movement (phase 1) from the internal approach

Figure 3 shows some field collected images depicting two of the origin destination paths. In Figure 3a, phase 6 (origin 1) at the north intersection is active (callout “i”). The car in the southbound thru lane (callout “iii”) will continue over the southbound thru advanced detector (callout “iv”) and leave the intersection via overlap-D (destination 1). The car in the left lane (callout “v”) will pass over the southbound left advanced detector (callout “vi”) and leave the intersection via phase 1 (destination 2). These vehicle arrivals can be correlated with the green/red status of the corresponding destination phase at the south intersection.

In Figure 3b, phase 7 (origin 2) at the north intersection is active (callout “vii”). A red truck (callout “ix”) will proceed over one southbound thru advanced detector (callout “x”) and a silver truck (callout “xi”) will proceed over the other southbound thru advanced detector (callout “xii”). Both of these vehicles will leave the intersection via the southbound thru movement, overlap-D (destination 1).

Absent from Figure 3 is an example of a vehicle from the WB exit ramp phase 7 (origin 2) exiting the south intersection via the SBL movement or phase 1 (destination 2). While this U-turn movement is valid (exiting the interstate and reentering in the opposite direction), relatively few vehicles execute this maneuver compared to the portion of vehicles from the ramp proceeding southbound through overlap-D, as will later be documented in subsequent figures.

## INTERIOR TRAJECTORY ANALYSIS USING HIGH RESOLUTION DATA

Figure 3 was used to illustrate the operation of the internal approach of the south intersection. From the advanced detectors, with two upstream origin phases (phase 6 and phase 7) and two downstream destination phases (overlap-D and phase 1), there are four paths of interest. Ideally, each of those four movement paths has vehicles arriving at the corresponding destination movement when the signal is green. As shown in Figure 1, the advanced detectors on the internal approaches are 295’ back from the intersection. The posted speed of 40 MPH makes this about 5 seconds from the stop bar. When a vehicle is detected, the signal status of the downstream intersection 5 seconds later is of interest. For example, a vehicle detection at 9:40:32 would use the signal status at 9:40:37 to determine whether the signal was green or red at the time of arrival at the stop bar. Performance measures for identifying queues are discussed later in this paper.

In Figure 4a, callout “i” shows a line where vehicle detections from the high-resolution data will be plotted. The line represents approximate travel time from the North INT to the South INT. The south INT shows which phase is active for Ring 1. Since Figure 4a is observing southbound thru vehicles, overlap-D is of particular interest. The line for overlap-D is green whenever either of its parent phases (phase 1 or phase 2) is active. The detections are projected forward by approximately 5 seconds, showing the status of overlap-D (destination 1) when those detections likely arrive at the stop bar. The detections are also projected upward and to the left by a static offset value of 10 seconds (the field measured and video-confirmed travel time from the

upstream stop bar to the interior advanced detector), showing the likely upstream source phase at the north INT. Callout “ii” highlights a group of detections representing a platoon. When projected forward by 5 seconds, these vehicles arrive at the downstream signal on overlap-D green (callout “iii”); when projected upstream by approximately 10 seconds, they are calculated to source from phase 6 (callout “iv”). Similarly, callout “v” shows a group of vehicles that arrive at the downstream signal on overlap-D green (callout “vi”) and that source from phase 7 (callout “vii”). Callout “viii” notes a distinct gap between the two platoons in the next cycle which more clearly shows how each platoon is associated with its upstream source phase.

This concept is also applied to the internal approach of the south INT for the southbound left, phase 1 (destination 2) in Figure 4b. Note that there is an absence of any vehicles sourced from the upstream WB ramp, phase 7. As previously mentioned, the U-turn movement from the interstate contributes very little traffic to the SBL arrivals at the south intersection. Figure 4c and Figure 4d also show this for the north INT thru and left, respectively, again having zero NBL vehicles (phase 5) sourced from the EB ramp (phase 3) in Figure 4d.

These figures illustrate the importance of ring displacement. In Figure 4a and Figure 4b, increasing the ring displacement would slide the north INT band to the right, thus also sliding the detections to the right. The detections would then be projected to new locations on the band for the south INT. Additionally, increasing the ring displacement would slide the north INT band to the right in Figure 4c and Figure 4d, affecting how NB vehicles (from the south INT) would arrive at their destinations; the NB vehicles coming from the south INT would arrive earlier at the north INT. These changes could drastically change the quality of progression and driver perception of operations.

### **VISUALIZING SOURCE MOVEMENTS PROGRESSING THROUGH THE INTERIOR**

To expand the Figure 4 concepts over more cycles or even an entire plan period, the Purdue Coordination Diagram (PCD) (12) provides an important visualization tool of the projected stop bar arrival trends (projected downstream from the advanced detector by 5 seconds). Figure 5a encompasses the same time period as Figure 4a, but covers 15 cycles. In Figure 5a, callout “i” denotes the start of the green of overlap-D and callouts “ii” and “iii” denotes platoons from upstream source phases 6 and 7 (respectively). Callout “iv” indicates the termination of overlap-D. On the next cycle, one vehicle (callout “v”) arrives before the start of green, and the rest of the platoon follows, arriving during green. Callout “vi” shows an instance where overlap-D runs continuously for two cycles, as there was no call on the EB ramp (this is also documented in Figure 4 where the south INT band serves phase 1, phase 2, phase 1, phase 2, and then phase 3). An interesting note is callout “vii” which shows the start of overlap-D red that clipped 4 cars (callout “viii”) at the end of a platoon originating from the upstream ramp.

Figure 5b shows the PCD concept for the southbound left turn (phase 1). Callout “ix” shows a platoon of vehicles that just missed the previous green that gapped out and instead arrived very early after the start of red, and consequentially have a long delay. Callout “x” shows a few vehicles from the upstream ramp (phase 7) which would suggest these are U-turning vehicles. As previously mentioned, there are relatively few vehicles making this movement.

Figure 6 shows the PCDs for both the SB thru (overlap-D) and the NB thru (overlap-H) over the entire plan period from 0900-1400. Clearly, most vehicles arrive within the green band (i.e. detection events occur between the green and red line). Finally, Figure 7 shows the PCD for both thru movements over 24 hours. The change in sequence from one pattern to another is quite evident. For example, in Figure 7a, pattern 2 from 0600-0900 shows vehicles from the upstream ramp (phase 7) arriving in the green band for the SB thru overlap-D first (callout “i”), followed



by vehicles from the SB thru (phase 6) vehicles (callout “ii”). This sequence is reversed in pattern 1 between 0900 and 1400, where the SB thru vehicles (callout “iii”) arrive first and are followed by vehicles from the ramp (callout “iv”). Callout “v” indicates a portion of the green band where there are no SB vehicles arriving on OL-D for the entirety of pattern 2 (wasted green time). The NB thru (phase 2) is the heavy movement that is keeping OL-D active.

## NUMERICAL INTERCHANGE PERFORMANCE MEASURES

To determine if the ring displacement parameter is tuned correctly, or if it needs adjustment, there needs to be a way to quantify the performance at the interchange. Historically, travel time has been used. However, this data is typically expensive to obtain, and difficult to interpret over short ranges such as within a diamond interchange. Using the high-resolution event based detector and phase data, there is an opportunity to develop performance measures that evaluate the progression of all vehicles in every movement, on a cycle-by-cycle basis.

The data consists of a list of  $N$  vehicle detection times projected downstream to the stop bar  $D_i$ , where  $i = 1, 2, \dots, N$ ; a list of  $M$  start of green times  $G_j$ , where  $j = 1, 2, \dots, M$ ; and a list of  $L$  start of red times  $R_k$ , where  $k = 1, 2, \dots, L$ . For each vehicle arrival time it is possible to find the most recent start of green from

$$G_i = \max(G_j) \quad \forall G_j \leq D_i \quad \text{Eq. 1}$$

The time of the most recent start of red event is

$$R_i = \max(R_k) \quad \forall R_k \leq D_i \quad \text{Eq. 2}$$

A vehicle is an arrival on green if  $G_i > R_k$ . For each arrival time, it is possible to define the following arrival function where  $A_i = 1$  for an arrival on green and  $A_i = 0$  for an arrival on red.

$$A_i = \begin{cases} 0, & G_i < R_i \\ 1, & G_i > R_i \end{cases} \quad \text{Eq. 3}$$

The total number of arrivals on green is therefore

$$N_g = \sum_{i=1}^N A_i \quad \text{Eq. 4}$$

and the overall percent on green (POG) is

$$P = \frac{N_g}{N} * 100 \quad \text{Eq. 5}$$

The quality of progression can be assessed with  $P$  (eq. 5). For example, in Figure 7a for pattern 2 between 0900 and 1400, the number of southbound thru vehicles that arrive on green (number of dots between the green line and red line) is 4,161 ( $N_g$ ). The number of arrivals on red (number of dots between the x-axis and green line) is 327. Thus, of the total 4,488 vehicles ( $N$ ), the POG is 93% ( $P$ ). This measured value is plotted in Figure 8a.

In Figure 7b, for pattern 2 between 0900 and 1400,  $N_g = 2,177$  and  $P = 85\%$ . This value is also plotted in Figure 8a. The POG for the NBL (57%) and SBL (53%) movements are also plotted on Figure 8a. The intersection as a whole achieved 80% POG which is plotted at  $x=0$  in Figure 8b. Looking at the curves, this is the global maximum which indicates that the intersection is working quite well for the programmed sequence.

## OPTIMIZATION OF RING DISPLACEMENT

With a quantifiable metric established, superposition of detector arrivals on the PCDs can be used to predict the ring displacement effect on POG. For example, if the ring displacement parameter is decreased by 10 seconds for this period (meaning that the start of the coordinated phase for the north intersection would occur ten seconds earlier), the POG for each of the movements changes accordingly to Figure 8a at  $x = -10$ ; all of the POG values decrease. The intersection as a whole is predicted to achieve a POG of 69%. An adjustment of  $x = +10$  yields a predicted POG of 74%.

This prediction was validated by a field exercise. The ring displacement was adjusted by -10 seconds in the field on July 10, 2013, and the subsequently measured POG was 71%. When the ring displacement parameter was adjusted +10s in the field on July 11, 2013, the measured POG was 69% (Figure 8b). The predicted trends closely match the measured results from field adjustments.

The predicted and observed values shown in Figure 8b are not identical because the system is not exactly linear, and there is stochastic variation in traffic. However, they are close enough to provide a reliable performance measure for evaluating whether or not ring displacement adjustments are warranted.

## Visualization of Ring Displacement Tuning Using Flow Profiles

The results of this field exercise are documented using flow profile diagrams in Figure 9. For each cycle, the probability of green is represented by the green area on the graphs. Vehicle arrivals from the upstream thru movement and upstream ramp are represented by black and gray bars respectively. Ideally, most vehicle arrivals would occur during a portion of the cycle when the probability of green is high. For the base scenario, the SBT (Figure 9a) works well; the NBT (Figure 9b) also has good progression, save for the tail of the platoons from the upstream ramp (callout “i”).

When ring displacement was set to 32 ( $\Delta = -10$ ), the leading SBT platoon arrived slightly early of the green window (Figure 9c, callout “ii”). The upstream green band was shifted 10 seconds earlier, causing northbound ramp vehicles to arrive in red (Figure 9d, callout “iii”).

When ring displacement was set to 52 ( $\Delta = +10$ ), the SBT vehicles arrived later in the green band at the south intersection, and the ramp platoon experienced significant arrivals on red (Figure 9e, callout “iv”). Since the green band for the north intersection is shifted to the right, the leading NBT vehicles from the south intersection arrive early (Figure 9f, callout “v”).

## IDENTIFYING EXCESSIVE INTERIOR QUEUEING

High occupancy of the interior advance detectors indicates the presence of queue spillback (13). Figure 10a shows the occupancy during red for the SBL advanced detector. Callout “i” shows an instance where the advance detector was occupied for 92% of the time during red, indicating a queue that reached the detector. In Figure 10b, the SBT phase at the north intersection is active (callout “ii”), but the queue has spilled back to the south intersection (callout “iii”). In Figure 10c, the signal turns yellow (callout “iv”); the truck (callout “v”) attempts to proceed and blocks the NBL ramp vehicle (callout “vi”). The intersection is jammed until the SBL phase becomes active and the queue dissipates. In this study, this occurrence was seldom and not easily distinguishable in the PCDs which cover hundreds of cycles.

Advanced detectors’ occupancy on red is an important performance measure which can be used to flag intersection lockup conditions. Using more fidelity on the queue estimates is possible using techniques proposed by Liu et al.

## **IDENTIFYING RAMP QUEUING**

Queues on ramps are particularly problematic at diamond interchanges. In Figure 11a and Figure 11b, neither right turn advance detector is substantially occupied during red. However, in Figure 11c and Figure 11d, there are several instances where there is high detector occupancy for both left turn lanes. Lane “A” and lane “B” have occupancy above 50% during 48 and 29 cycles respectively.

The advance queue detectors on the ramps (Figure 1) are further upstream and can also be examined in the high resolution data. These detectors are tied together on a single channel and have a delay in the detector amplifier of 5.0 seconds. Each detector call represents when the queue is beginning to reach the freeway. The inset graph in Figure 11e shows 5 events where the queue detectors were active. This is very important information to operations personnel concerned with avoiding queue spillback onto the freeway. Using these queue detectors, the controller could be configured to call an off-ramp clearance preemption plan.

## **CONCLUSIONS**

High-resolution controller event data is a valuable tool in measuring and assessing performance at diamond interchanges. This study demonstrated the use of high resolution controller data in the following applications:

- Diamond operation was visualized over several hours and multiple plans. This is particularly important because it is frequently impractical to allocate staff time for that purpose, and for many large diamond interchanges, it is often difficult to find a vantage point to make high quality observations. The paper provided example PCDs (Figure 5, Figure 6, and Figure 7) and flow profiles (Figure 9) as visualizations that would be suitable for controller front panel display or central system graphics.
- Quantitative performance measures were developed to assess the quality of progression for the four external movements (Figure 8a), and demonstrate how those could be used to verify whether the settings are appropriate, or initiate a ring displacement parameter change. Figure 8b demonstrated that the predicted and observed values of POG for ring displacement adjustments were in reasonable agreement.
- Performance measures were defined for evaluating how effectively the interior of the diamond interchange was clearing. It was shown that high red occupancy ratios correlated with excessive interior queuing (Figure 10). These same performance measures can be used to evaluate risk of ramps queuing onto the interstate (Figure 10e).

A final important note is that the performance measures demonstrated in this paper depend upon appropriate detection configurations. As high-resolution data and performance measures become vital engineering tools, it is critical that diamond interchange designs include advanced detection at all approaches. As the detection practices are adopted, modern controllers with graphical displays, or the ability to provide such a display on a mobile device, would be ideal platforms to convey this information to engineers in the field.

## ACKNOWLEDGEMENT

This work was supported by the Indiana Department of Transportation. The contents of this paper reflect the views of the authors, who are responsible for the facts and the accuracy of the data presented herein, and do not necessarily reflect the official views or policies of the sponsoring organizations. These contents do not constitute a standard, specification, or regulation.

## WORKS CITED

1. Pinnell C, Capelle DG. Design and Operation of Diamond Interchanges. College Station: A. & M. College of Texas, Texas Transportation Institute; 1961. Report No.: E-45-61.
2. Chaudhary NA, Chu CL. Guidelines for Timing and Coordinating Diamond Interchanges with Adjacent Traffic Signals. College Station: The Texas A&M University System, Texas Transportation Institute; 2000. Report No.: TX-00/4913-2.
3. Fambro DB, Bonneson JA. Optimization and Evaluation of Diamond Interchange Signal Timing. ITE Compendium of Papers. 1988; 125.
4. Koonce P, Bullock D. Evaluation of Diamond Interchange Signal Controller Settings by Using Hardware-In-The-Loop Simulation. Transportation Research Record. 1999; 1683.
5. Herrick GC, Messer CJ. Strategies for Improving Traffic Operations at Oversaturated Diamond Interchanges. College Station: The Texas A&M University System, Texas Transportation Institute; 1992. Report No.: FHWA/TX-92/1148-4F.
6. Smaglik EJ, Sharma A, Bullock DM, Sturdevant JR, Duncan G. Event-based data collection for generating actuated controller performance measures. Transportation Research Record. 2007; 2035.
7. Sturdevant JR, Overman T, Raamot E, Deer R, Miller D, Bullock DM, et al. Indiana Traffic Signal Hi Resolution Data Logger Enumerations. West Lafayette: Purdue University, Indiana Department of Transportation; 2012. Report No.: <http://dx.doi.org/10.5703/1288284315018>.
8. Munjal PK. An Analysis of Diamond Interchanges. Transportation Research Record. 1971; 349.
9. Engelbrecht RJ, Barnes KE. Advanced Traffic Signal Control for Diamond Interchanges. TRB Annual Meeting CD. 2003.
10. Venglar S, Koonce P, Urbanik, II T. Passer III-98 Application and User's Guide. Guide. College Station: Texas A&M University System, Texas Transportation Institute; 1998.
11. Nelson EJ, Bullock D, Urbanik T. Implementing Actuated Control of Diamond Interchanges. Journal of Transportation Engineering. 2000; 126.
12. Brennan, Jr. TM, Day CM, Sturdevant JR, Bullock DM. Visual Education Tools to Illustrate Coordinated System Operations. Transportation Research Record. 2012 February; 2259.
13. Liu HX, Wu X, Ma W, Hu H. Real-time queue length estimation for congested signalized intersections. Transportation Research Part C. 2009; 17.

**LIST OF TABLES**

Table 1 Day plan for the diamond interchange.....	14
---	----

**LIST OF FIGURES**

Figure 1 I-465 @ SR-37 Diamond Interchange layout and phasing.....	12
Figure 2 Patterns and Sequences to scale with Ring Displacement shown. Note that Ring 1 pertains to the south intersection and is on the bottom. ....	13
Figure 3 Field images of platoon sources based on the upstream signal status.....	15
Figure 4 Sequence of HiResolution data events at the interghance including phase status and detector information.....	16
Figure 5 Purdue Coordination Diagram showing cycle-by-cycle information and identifying upstream source phase .....	17
Figure 6 Purdue Coordination Diagram showing an entire plan from 0900-1400 on Wednesday, June 5, 2013 .....	18
Figure 7 Purdue Coordination Diagram showing entire 24 hours on Wednesday, June 5, 2013	19
Figure 8 Ring displacement sweep results.....	20
Figure 9 Flow Profile Diagrams, relative to green, for the internal thru movements for varying ring displacement (-10 / 0 / +10) values for pattern 3 from 0900-1400 .....	21
Figure 10 Red occupancy profiles and visual confirmation from the north intersection looking south at the back of the SB Left queue .....	22
Figure 11 WB Ramp detector occupancy .....	23

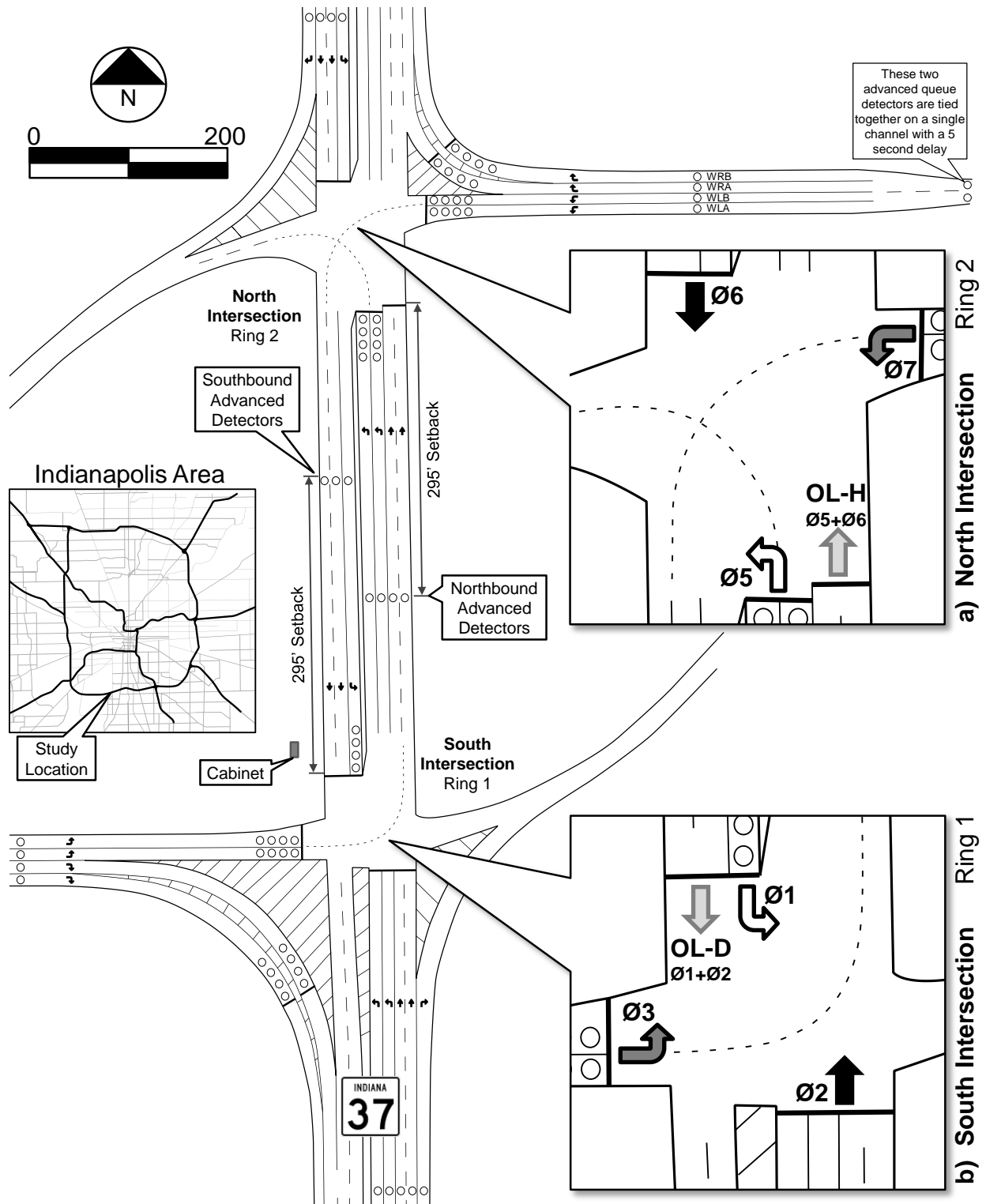
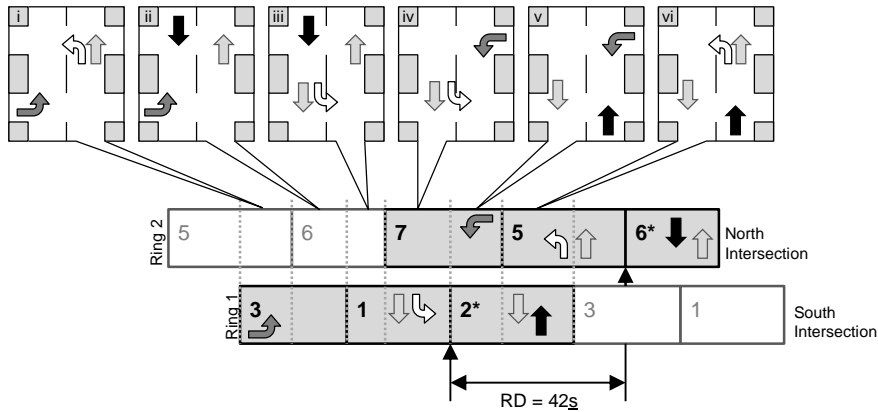
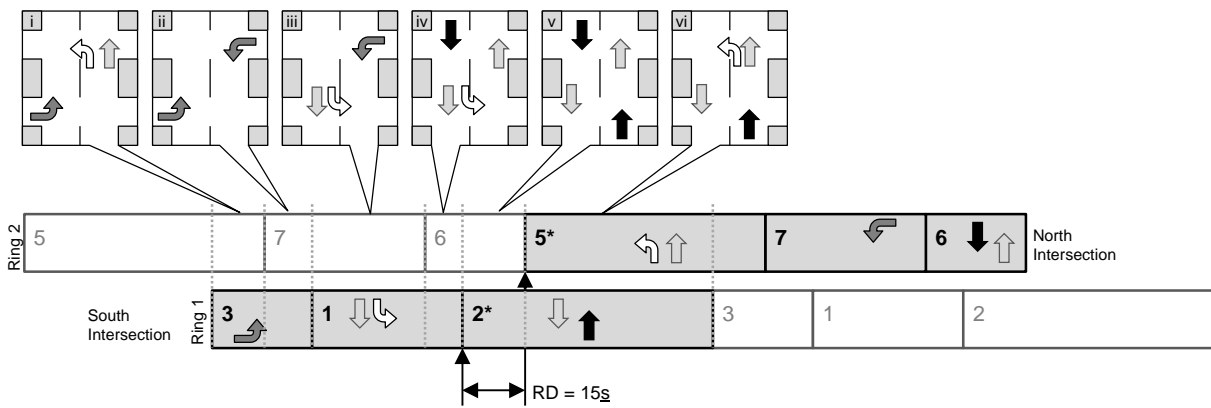


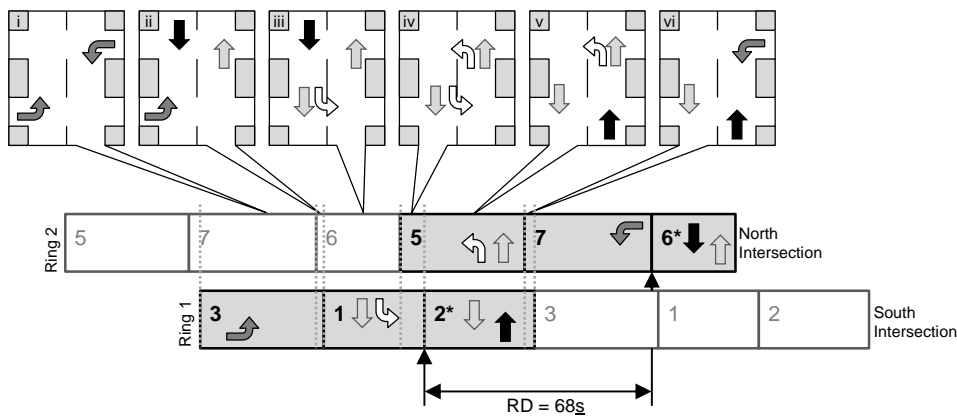
Figure 1 I-465 @ SR-37 Diamond Interchange layout and phasing



**a) Pattern 1, Sequence 2, Cycle Length = 80s, RD = 42s**



**b) Pattern 2, Sequence 1, Cycle Length = 120s, RD = 15s**



**c) Pattern 3, Sequence 2, Cycle Length = 80s, RD = 68s**

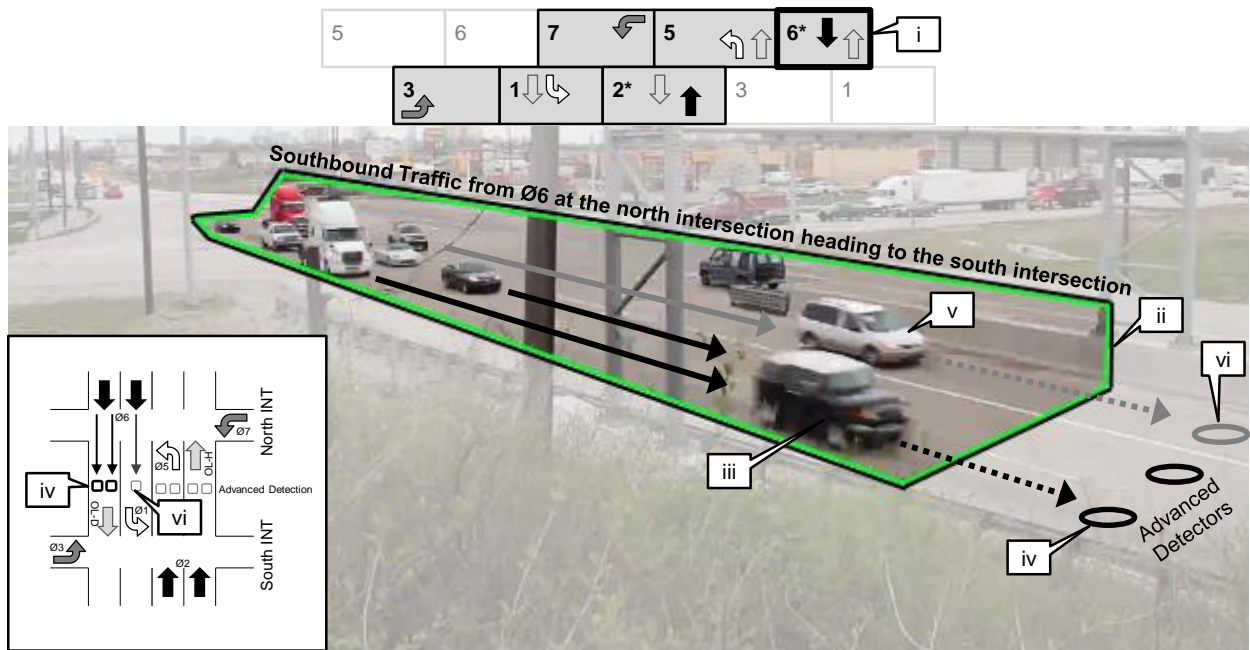
Figure 2 Patterns and Sequences to scale with Ring Displacement shown. Note that Ring 1 pertains to the south intersection and is on the bottom.

*\*Indicates coordinated movement*

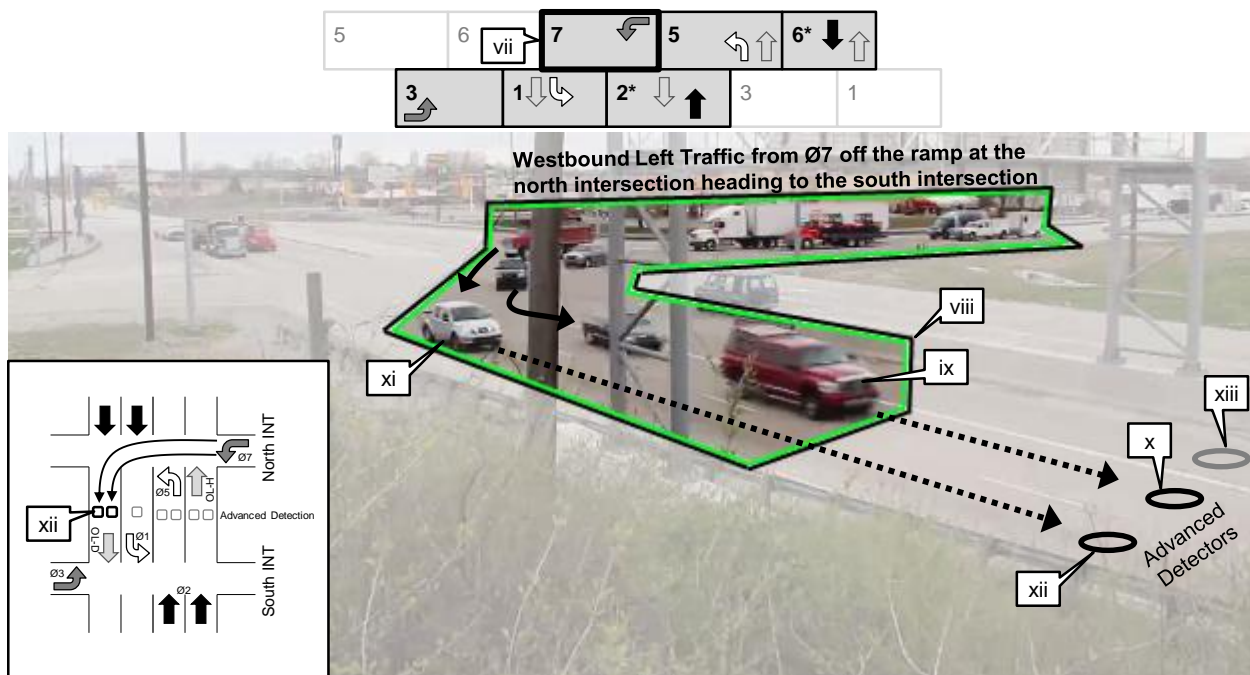
Table 1 Day plan for the diamond interchange

Start	End	Pattern	Seq ID	Cycle Length Sequence(seconds)	Ring Displacement (Seconds)	Coord. Movements	Notes
0000	0600	1	2	N:  7,5,6 S:  3,1,2	80	42 6 2	Off peak.
0600	0900	2	1	N:  5,7,6 S:  3,1,2	120	15 5 2	AM Peak period, heavy NB movement as traffic heads into the city. NBL is coordinated.
0900	1400	1	2	N:  7,5,6 S:  3,1,2	80	42 6 2	Mid-day pattern.
1400	1530	13	1	N:  5,7,6 S:  3,1,2	80	68 6 2	Same as pattern 3, but max recall on NBL.
1530	1900	3	1	N:  5,7,6 S:  3,1,2	80	68 6 2	PM peak period. Heavy traffic on the ramps heading south.
1900	0000	1	2	N:  5,7,6 S:  3,1,2	80	42 6 2	Off peak.



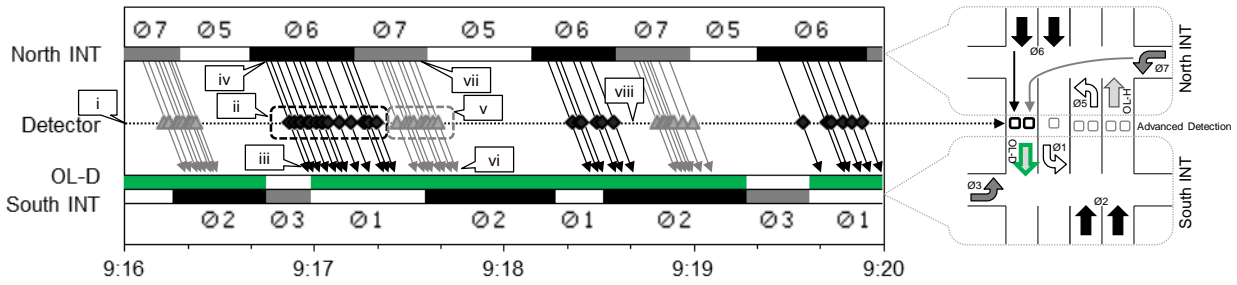


a) Vehicles heading southbound towards the advanced detector from the upstream thru movement

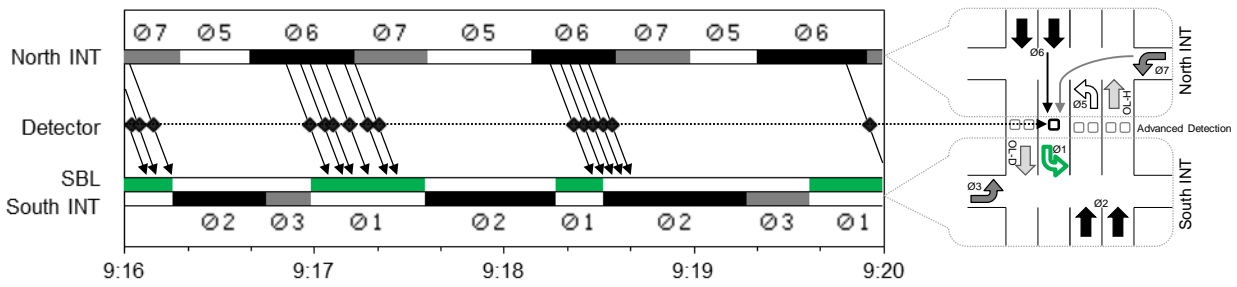


b) Vehicles heading southbound towards the advanced detector from the upstream left movement

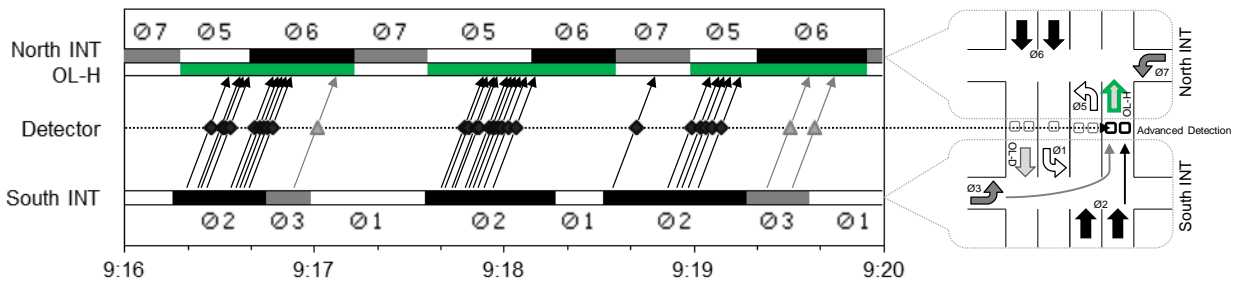
Figure 3 Field images of platoon sources based on the upstream signal status



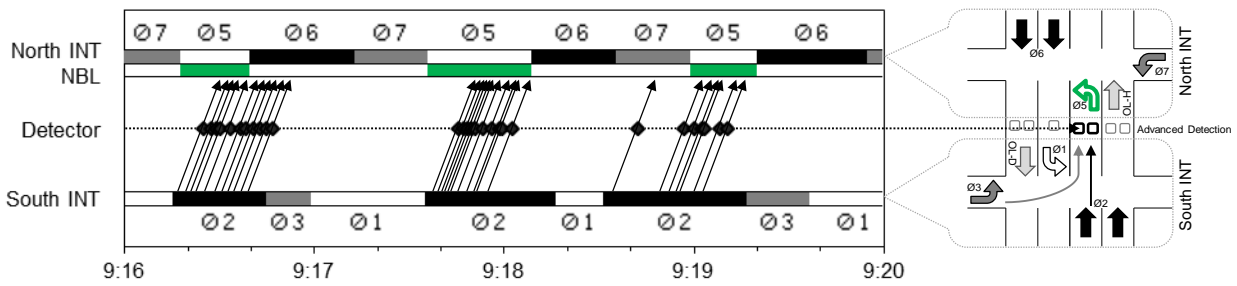
**a) Southbound thru traffic sourced upstream from Ø6 and Ø7 arriving at overlap-D (OL-D)**



**b) Southbound left traffic sourced upstream from Ø6 and Ø7 arriving at Ø1**

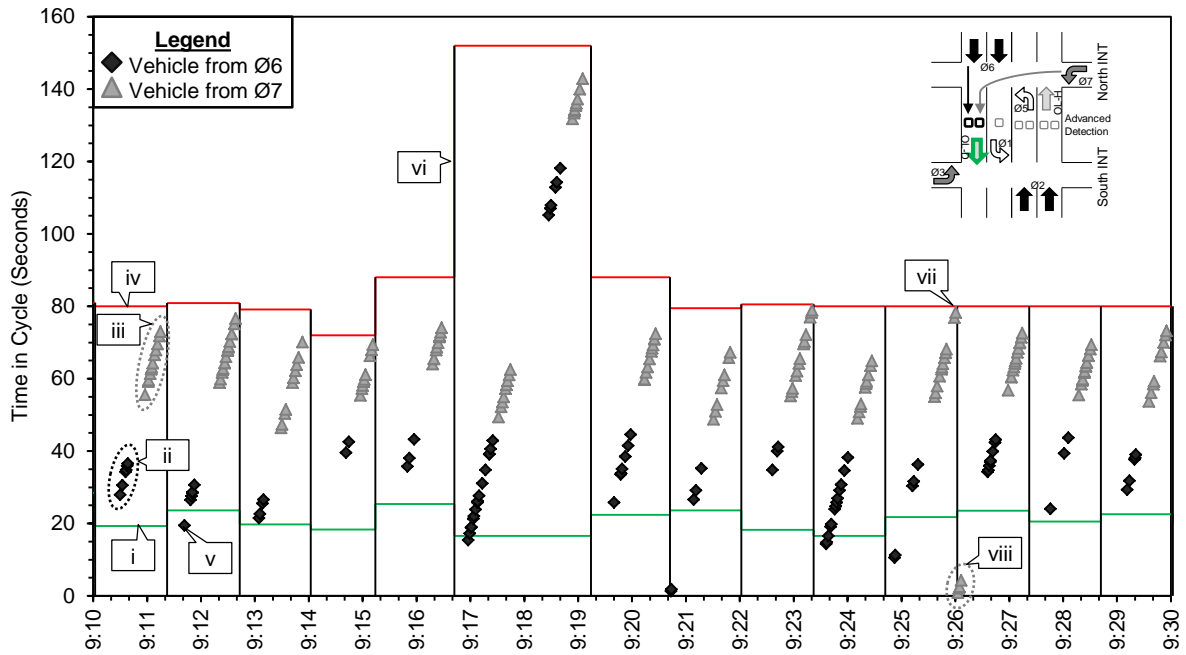


**c) Northbound thru traffic sourced upstream from Ø2 and Ø3 arriving at overlap-H (OL-H)**

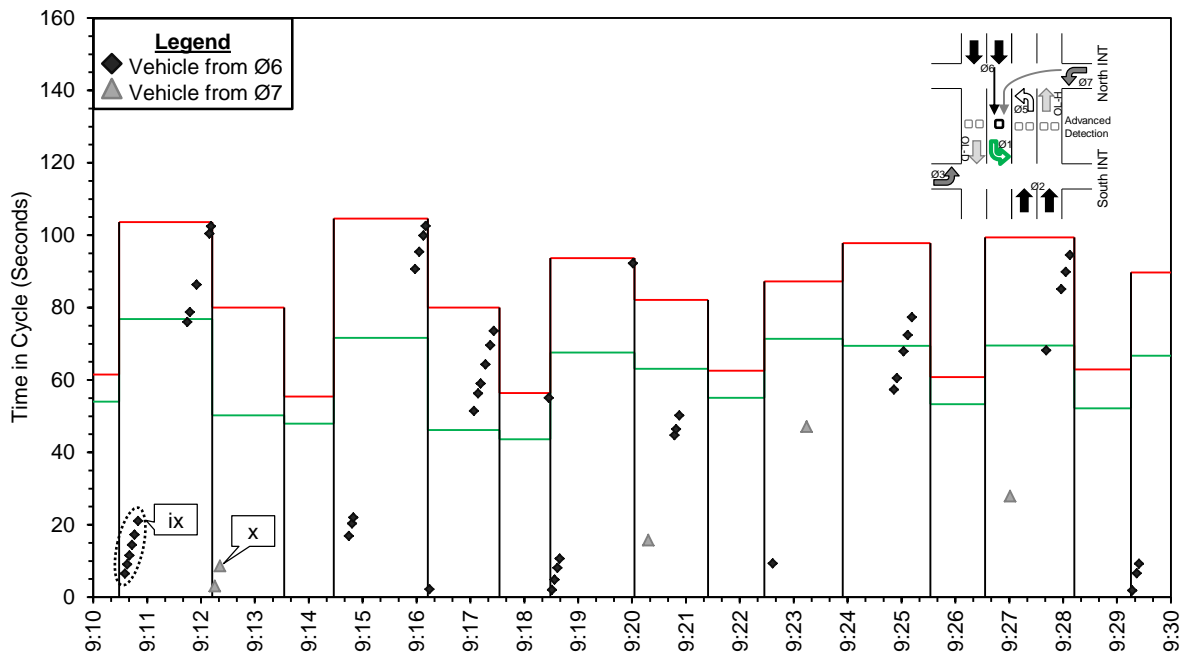


**d) Northbound left traffic sourced upstream from Ø2 and Ø3 arriving at Ø5**

Figure 4 Sequence of HiResolution data events at the interghance including phase status and detector information

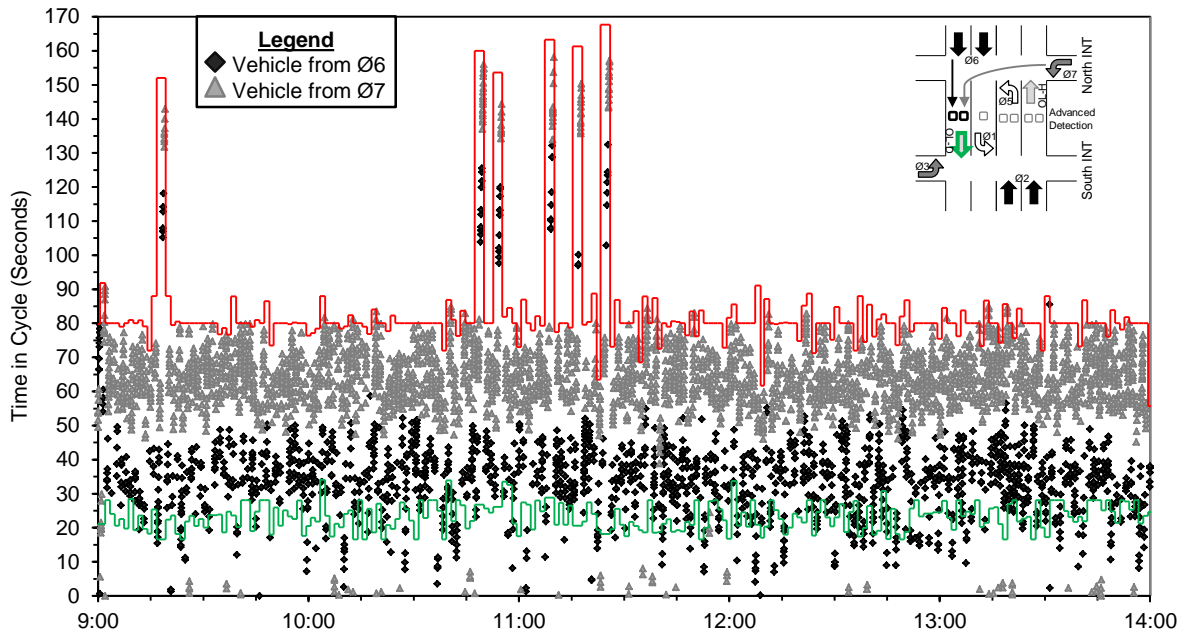


**a) Southbound Thru (Overlap - D)**

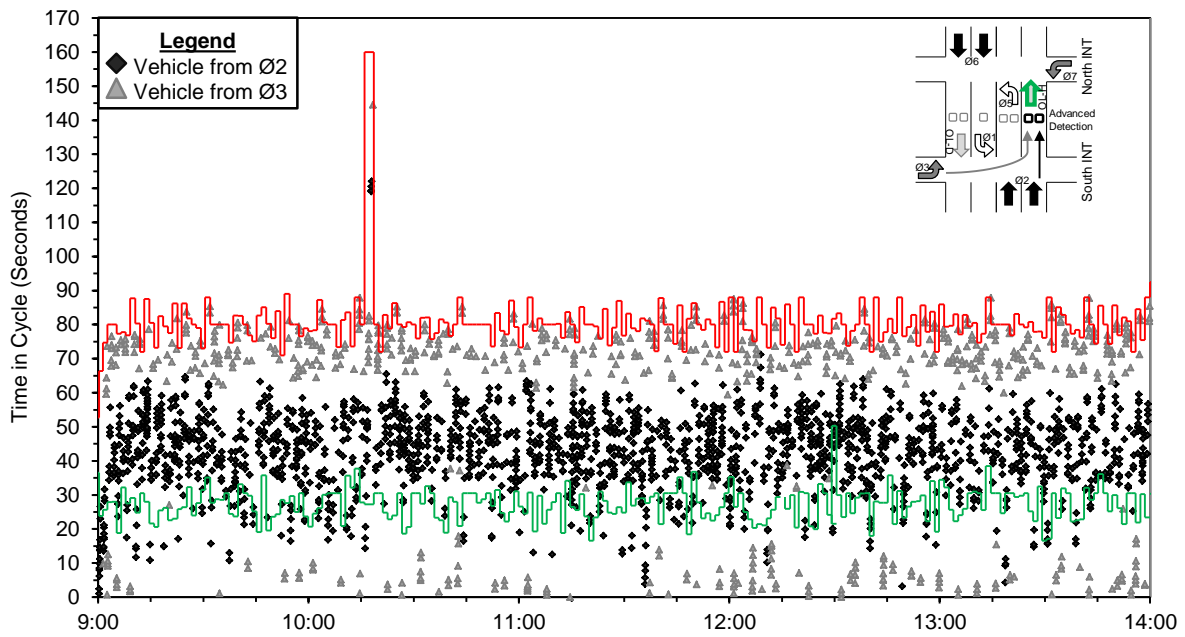


**b) Southbound Left (Phase 1)**

Figure 5 Purdue Coordination Diagram showing cycle-by-cycle information and identifying upstream source phase

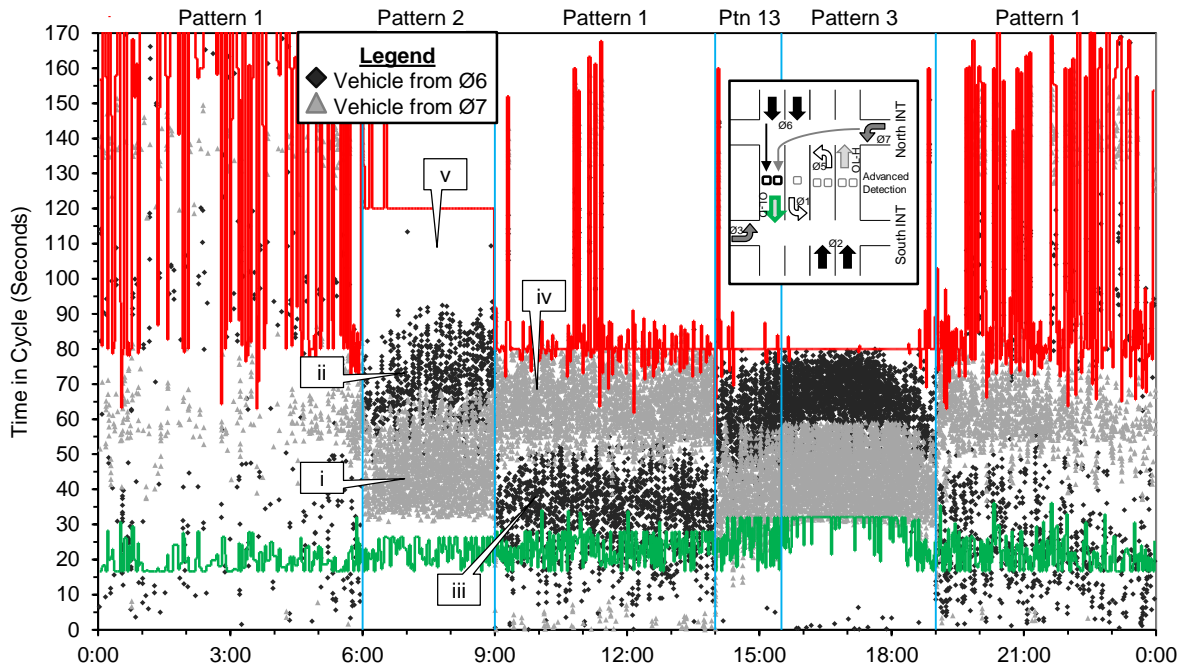


a) Southbound Thru (Overlap - D)

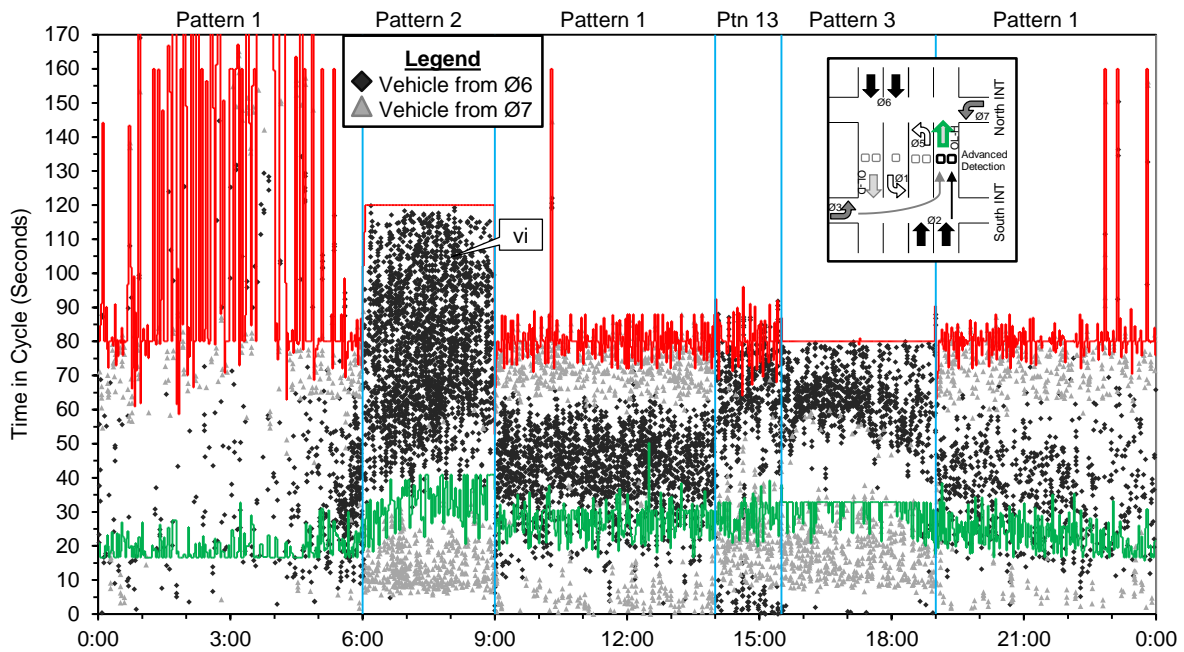


b) Northbound Thru (Overlap - H)

Figure 6 Purdue Coordination Diagram showing an entire plan from 0900-1400 on Wednesday, June 5, 2013

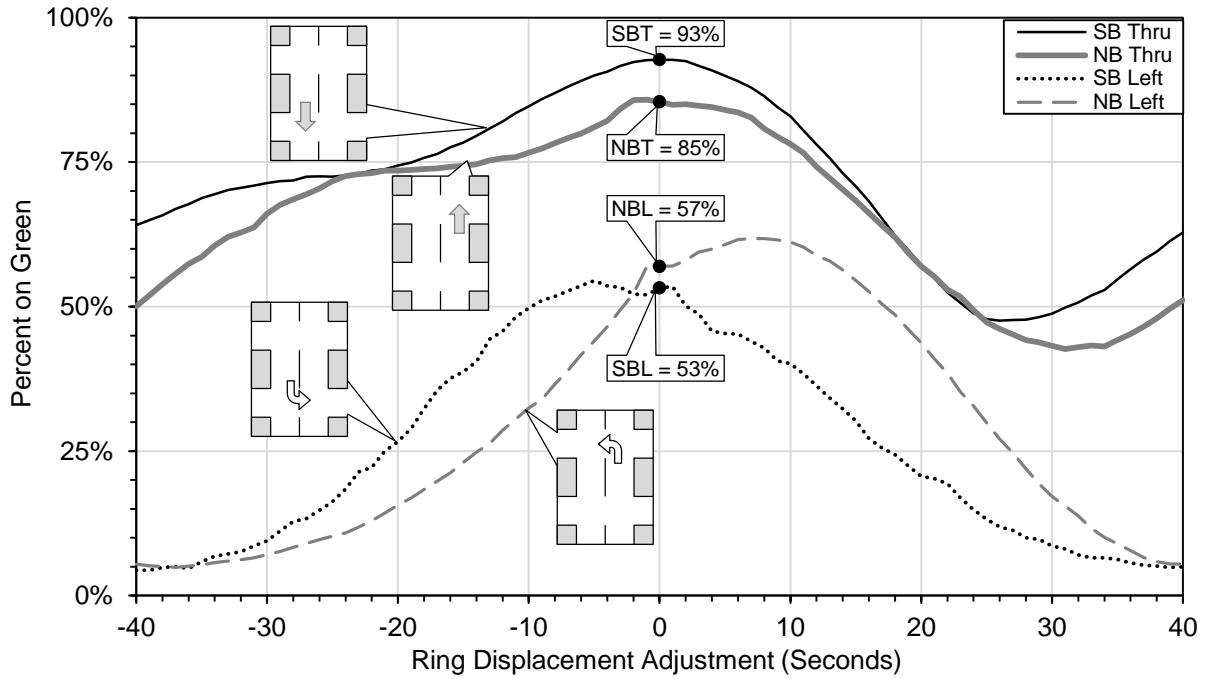


**a) Southbound Thru (Overlap – D)**

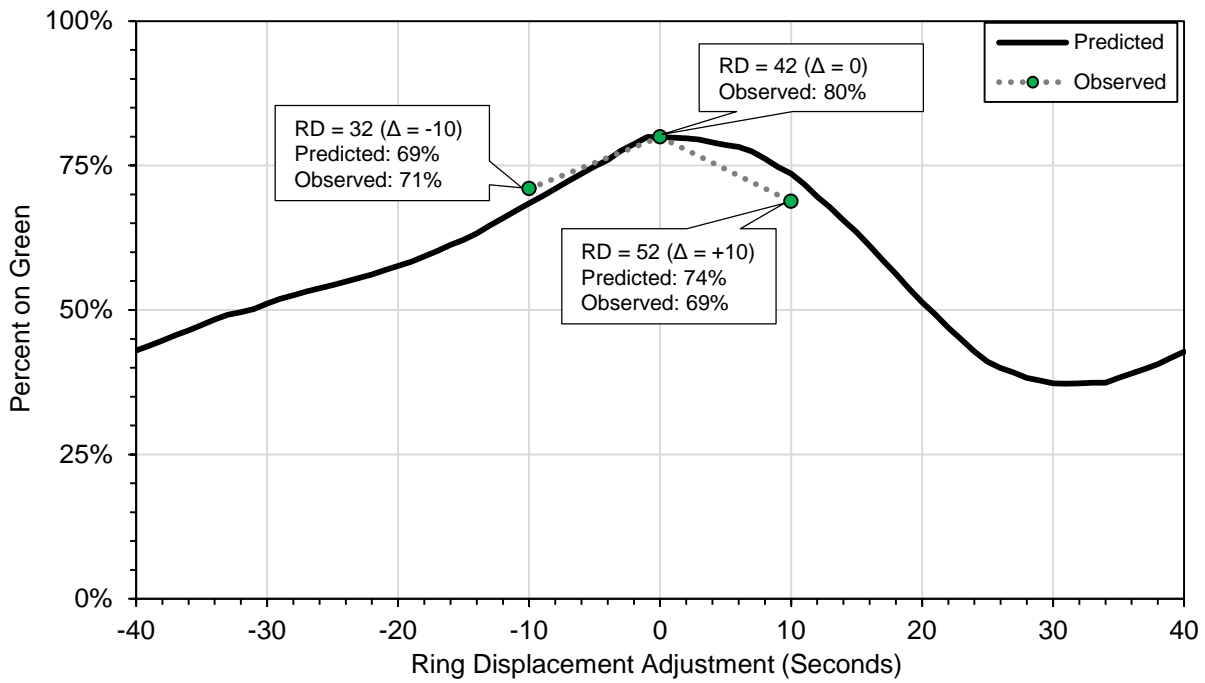


**b) Northbound Thru (Overlap – H)**

Figure 7 Purdue Coordination Diagram showing entire 24 hours on Wednesday, June 5, 2013



a) Predicted percent on green for four internal movements



b) Predicted composite percent on green for four internal movements with field observed measurements

Figure 8 Ring displacement sweep results



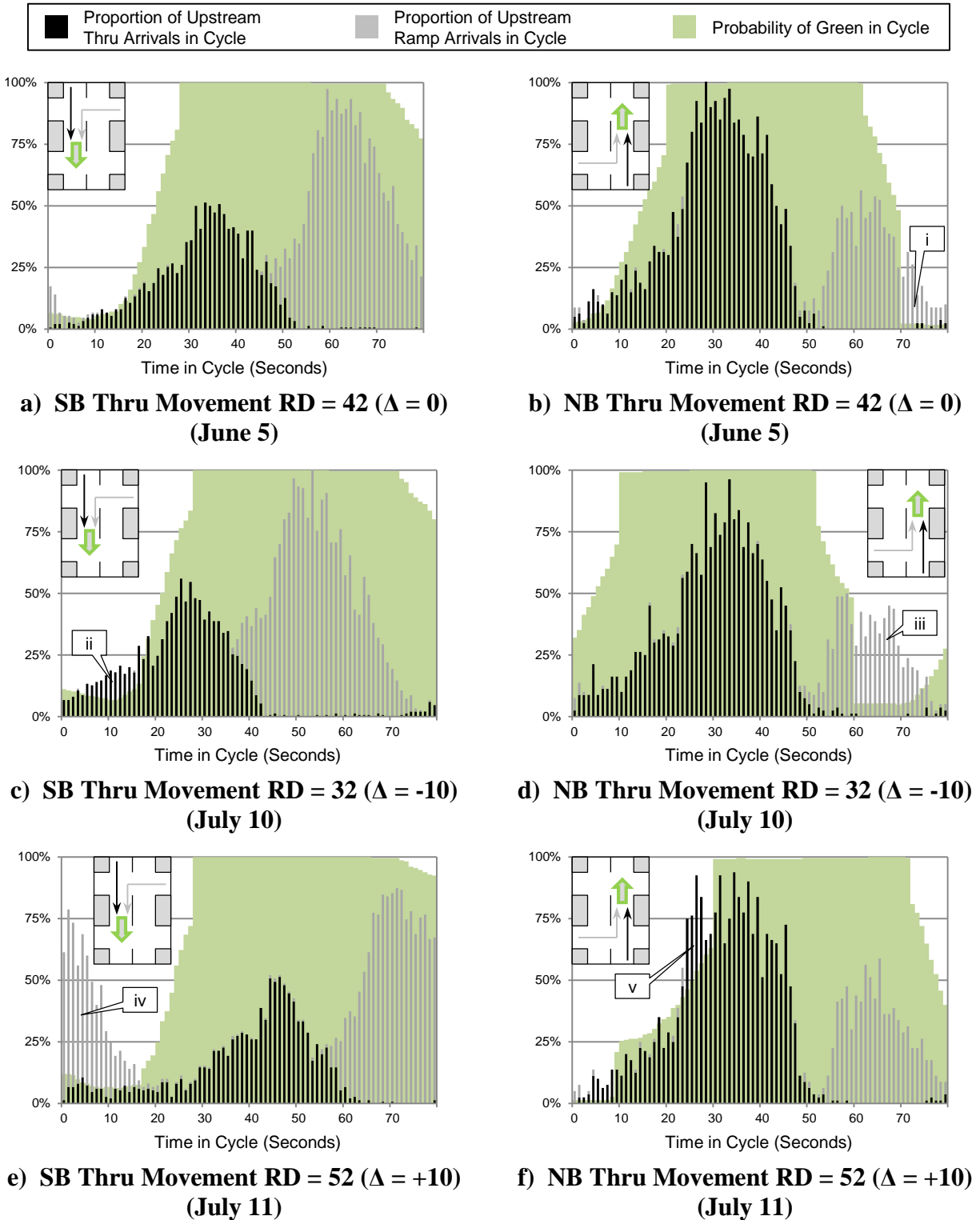
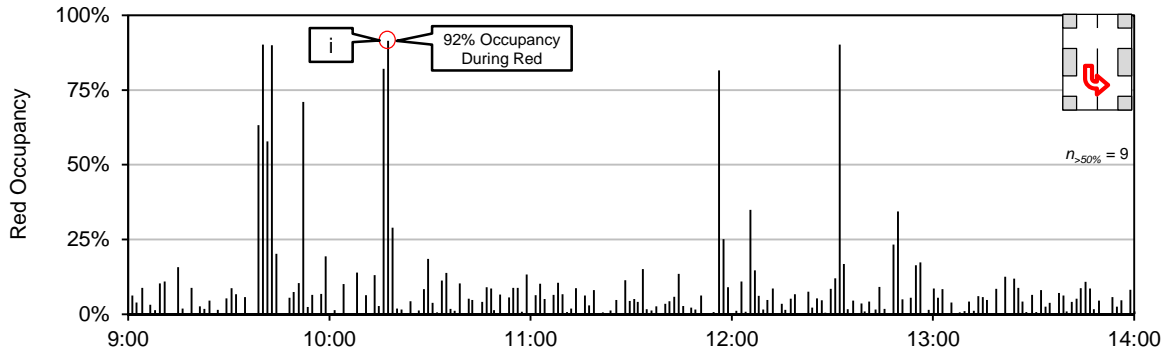


Figure 9 Flow Profile Diagrams, relative to green, for the internal thru movements for varying ring displacement (-10 / 0 / +10) values for pattern 3 from 0900-1400



**a) Red occupancy for SBL (Phase 1)**



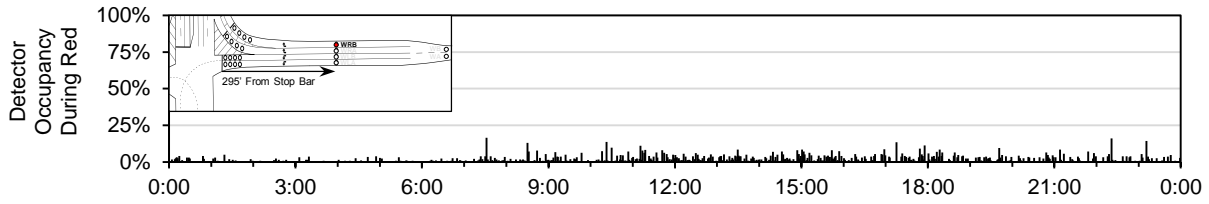
**b) SBL Queue at 10:17 just before yellow with a queue approaching critical length**



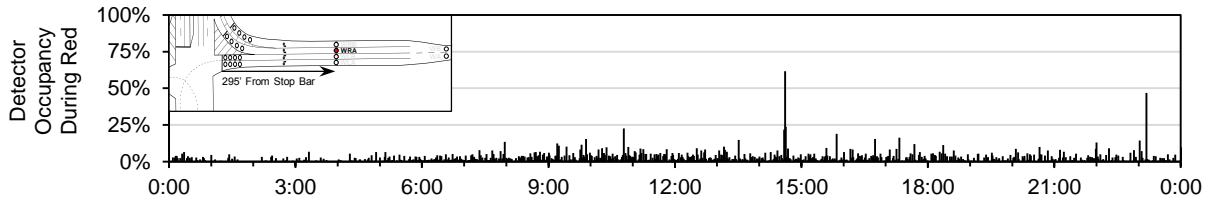
**c) SBL Queue at 10:17 during yellow. Entering vehicle is about to lock up the intersection**

Figure 10 Red occupancy profiles and visual confirmation from the north intersection looking south at the back of the SB Left queue

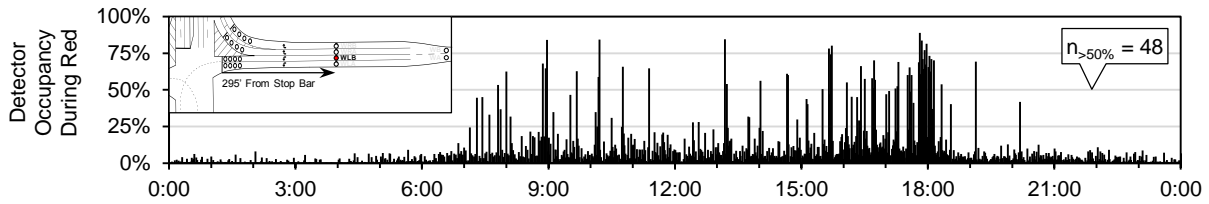




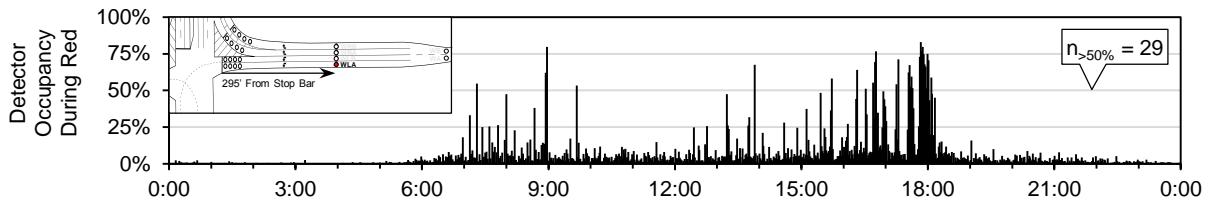
**a) WB Ramp Right Turn Lane B Detector Occupancy During Red**



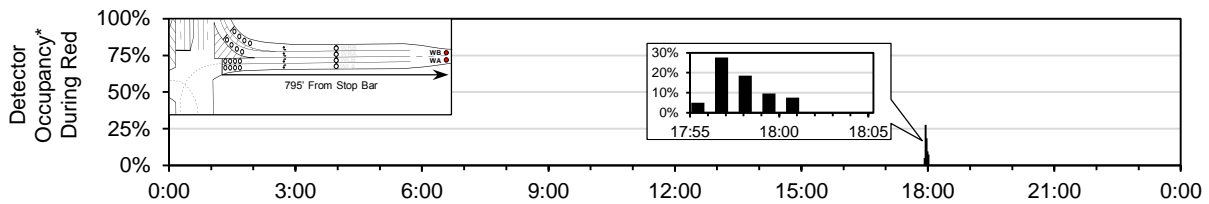
**b) WB Ramp Right Turn Lane A Detector Occupancy During Red**



**c) WB Ramp Left Turn Lane B Detector Occupancy During Red**



**d) WB Ramp Left Turn Lane A Detector Occupancy During Red**



**e) WB Ramp Advanced Queue Detector Occupancy\* During Red**

Figure 11 WB Ramp detector occupancy

\*Excluding the 5.0 second delay input to the controller